Signal Processing by Parametric Interactions in Delay-Line Devices

GORDON S. KINO, STEPHEN LUDVIK, H. J. SHAW, WILLIAM R. SHREVE, JAMES M. WHITE, AND DONALD K. WINSLOW

Invited Paper

***Abstract*—A new type of signal-processing device which employs the parametric interaction between surface or volume acoustic waves passing in opposite directions through an acoustic delay line is described. These devices are capable of giving the real-time convolution of two modulated signals, and the time inversion of an arbitrary signal. As one signal acts as the reference for the other, a virtually infinite range of electronically variable signal-processing functions, such as recognition of digital codes, pulse compression of an FM chirp, and the realization of a fast Fourier transform, is possible. Early devices which employed the nonlinearity of the acoustic medium tended to give outputs of the order of 60 dB less than the input signal. Recent developments, in which a semiconductor placed near the piezoelectric medium interacts with the acoustic wave, have yielded results where the loss from input to output is of the order of 30 dB.**

I. Introduction

When two signals are passed in opposite directions through an acoustic delay line, the nonlinearities in the system can give rise to a product signal at the sum frequency. Some years ago Svaasand [1], working with surface acoustic waves in a piezoelectric crystal, showed that the product signal can be detected electrically with simple electrodes distributed along the delay line. Wang [2], using bulk waves in a semiconducting crystal, showed that the modulation of the product signal is the convolution of whatever modulations exist on the two input signals. The convolution process was independently rediscovered later by Quate and Thompson [3], who passed longitudinal waves in opposite directions through $LiNbO_3$ and demonstrated the convolution of simple wave shapes. This type of signal processing was then demonstrated by Luukkala and Kino [4] using surface acoustic waves, and has since been observed and studied in a number of laboratories.

In this paper we shall mainly describe the work that has been carried out at Stanford University in this area, and will not attempt to give a complete survey of the many contributions made to the field in other laboratories. We have studied several aspects of this parametric interaction process. One aspect of our work has been to investigate the ways in which these devices can be used for signal processing of both digital and analog signals. In the former case we have used the basic convolution device to demonstrate accurate autocorrelation of digital signals such as biphase Barker codes [5]. For the analog case, we have demonstrated accurate pulse compression of symmetrical V–FM chirp signals [6]. In both cases the devices can handle wide variations in the signals and still accurately perform the convolution operation. We have also demonstrated that a modulated signal can be inverted in time using these devices. This is potentially of great importance for the case of analog signals, because it is a necessary step in the cross correlation of nonsymmetrical analog signals.

The basic properties of these devices and their advantages in signal-processing applications are now clear. When a signal is passed through a conventional filter, such as a bandpass circuit, the output from the system will be the convolution of the signal with the filter response function. In the usual surface acoustic wave filter, where the filtering in performed by a specially tapered transducer, the output is the cross correlation of the signal with the geometrical pattern of the transducer. If the transducer pattern is fixed, as it generally is for analog signals, the input signal can only be cross correlated with this fixed reference pattern.

In a parametric processor, on the other hand, one signal acts as a *reference* or filter for the other. Since the reference signal can be varied at will, the parametric convolutor is electronically variable. The convolution process takes place in real time, and the information capacity of the device, which is the product of the usable bandwidth and the time delay of the input signal along the active length of the device is of the order of 200 at the present time. However, with the use of the very long delay lines which are now being developed, it is expected that this parameter will eventually be increased by several orders of magnitude.

The device provides an additional advantage which is not available in fixed filter devices: a signal which has passed through a long path and suffered distortion could, in principle, be correlated with itself. Thus information about the nature and features of a particular signal, such as the details of a radar signal passing through the ionosphere, can be obtained. This information would be difficult to obtain with a fixed system.

The nonlinear interactions required for the operation of these devices occur directly in delay lines constructed of piezoelectric materials such as $LiNbO_3$. However, for many applications, the insertion loss of the normal piezoelectric devices tends to be too high. Consequently, it has been necessary to look for ways to increase the strength of the nonlinear coupling. One promising approach tried by Ash and his co-

Manuscript received October 4, 1972; revised November 2, 1972. This research was supported jointly by the USAF Systems Command, Rome Air Development Center, Griffiss AFB, Rome, N. Y., under Contract F3062(71-C)-0125; the U. S. Army Electronics Command under Contract DAAB07-71-C-0145; the U. S. Army Research Office–Durham under Contract DAHC 04-71-C-0005; the U. S. Office of Naval Research under Contract N00014-67-A-0112-0039.

The authors are with the Microwave Laboratory, Stanford University, Stanford, Calif.

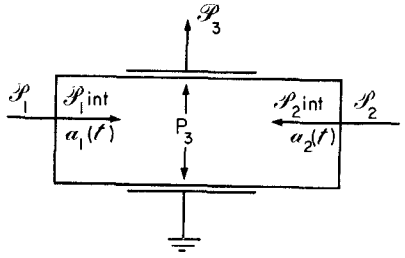

Fig. 1. Generalized parametric processor.

workers is to confine the acoustic beam to a narrow path in a surface "waveguide" [7]. This increases the power density and hence the strength of the nonlinear coupling. An alternative approach with which we have been experimenting is to use the stronger nonlinearities which can be obtained when a semiconductor is coupled to the RF electric field associated with an acoustic wave propagated along a piezoelectric delay line [2], [8], [11]. With the use of semiconductors one can obtain total insertion losses in the range of 30 dB, which should make it possible to apply parametric devices to a wide class of practical signal-processing systems.

II. Parametric-Wave Interactions

A. Convolution

In order to understand the basic signal-processing function of these parametric acoustic devices, we consider an acoustic delay line in which an acoustic wave $a_1(t)$ with a power $\mathcal{P}_{1\,int}=a_1a_1^*$ is inserted at one end (port 1) of a delay line, and a wave $a_2(t)$ with a power $\mathcal{P}_{2\,int}=a_2a_2^*$ is inserted in port 2 at the other end of the line, as shown in Fig. 1. The subscript int is used to refer to the power associated with the acoustic waves in the line. If no subscript is used, $\mathcal{P}$ refers to the electrical powers outside the device. At a point z along a lossless delay line, these signals have the form $a_1(t-z/v_A)$, $a_2(t-T+z/v_A)$, respectively, where T is the delay time of an acoustic signal from port 1 to port 2, and v_A is the acoustic wave velocity. Slight nonlinearities in the acoustic medium will give rise to a polarization density $\boldsymbol{P}_3(x, y, z)$ proportional to the product $a_1(t-z/v_A)a_2(t-T+z/v_A)$. In the special case when the two waves are CW signals of the form $a_1(t)=A_1\exp j\omega_1 t$, $a_2(t)=A_2\exp j\omega_2 t$, the RF fields associated with the polarization $\boldsymbol{P}_3$ will have components which vary as $\exp j(\omega_3 t-\beta_3 z)$, where

$$\omega_3 = \omega_1 + \omega_2 \tag{1}$$

$$\beta_3 = \beta_1 - \beta_2 = \frac{\omega_1 - \omega_2}{v_A}. \tag{2}$$

This signal may be detected by an output transducer designed to have a periodicity corresponding to the wave number β_3.

In both volume-wave and surface-wave devices of the types illustrated in Fig. 2(a) and (b), respectively, it is often convenient to work with a degenerate system in which the input frequencies are equal, i.e., $\omega_1=\omega_2=\omega$ and the output frequency is 2ω, with $\beta_3=0$. In this case the electric fields associated with $\boldsymbol{P}_3(z, t)$ are uniform with z, and may be detected between a pair of metal films deposited on the top and bottom surfaces of the delay line.

On the other hand, if the input signals have different frequencies, the wavenumber of the output signal is finite. In this

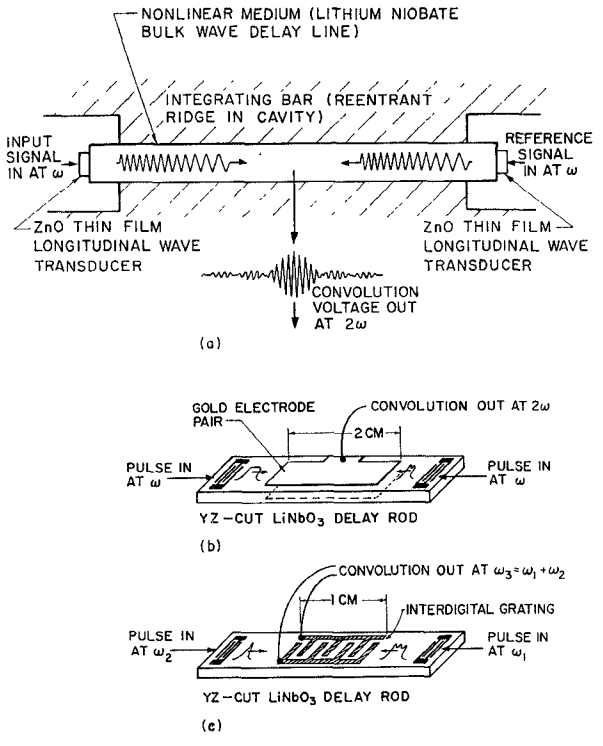

Fig. 2. Type of devices using piezoelectric nonlinearities. (a) Degenerate ($\omega_1=\omega_2$) bulk-wave device. (b) Degenerate surface-wave device. (c) Nondegenerate ($\omega_1\neq\omega_2$) surface-wave device.

case, it is convenient to work with acoustic surface waves and detect the output product signal on an interdigital transducer, as illustrated in Fig. 2(c), with a finger-pair period l where

$$\beta_3 l = 2\pi. \tag{3}$$

If the frequency difference between the two input signals is small, then $\beta_3 \ll \beta_1$ and β_2, and the output transducer will be much coarser, i.e., have a much longer period than either of the input transducers. Consequently, even when a relatively long output transducer is required, it is easy to fabricate.

It is important to realize that the output signal can be detected on the output transducer at any output frequency $\omega_3=\omega_1+\omega_2$, providing that $\omega_1-\omega_2$, i.e., $\beta_3=(\omega_1-\omega_2)v_A$, is kept constant. This is because the output transducer is phase sensitive rather than frequency sensitive. The implication is that when modulated signals are used, and ω_1 is changed to $\omega_1+\Delta\omega$, a strong output will be obtained if ω_2 is changed to $\omega_2+\Delta\omega$, i.e., if the modulation frequencies of the two input signals are the same. By a simple extension of Ramo's theorem [12], it can be shown that the induced current fed into a short-circuited output transducer due to the RF polarization current density $\boldsymbol{J}_3=j\omega\boldsymbol{P}_3$ is

$$I_{\text{out}} = \frac{1}{V_0}\int\int \boldsymbol{J}_3\cdot\boldsymbol{E}_0\, dz dA = \frac{j\omega_3}{V_0}\int\int \boldsymbol{P}_3\cdot\boldsymbol{E}_0\, dz dA \tag{4}$$

where $\boldsymbol{E}_0$ is the field in the acoustic medium produced by a voltage V_0 placed across the output transducer, and the integral is taken over the volume of the delay line. Thus we regard the output transducer as a current source, as shown in Fig. 3(a). It is often more convenient to view the output transducer as a voltage source, as shown in Fig. 3(b), with an open-

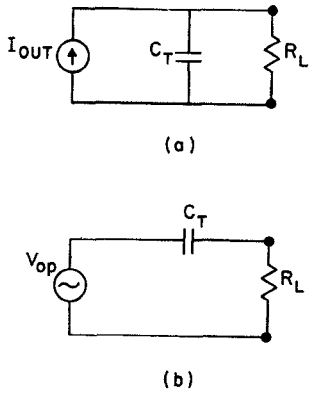

Fig. 3. Equivalent circuits for the output generated by the nonlinear piezoelectric devices. (a) Current-source representation. (b) Voltage-source representation.

circuit voltage V_{op} where

$$V_{op} = \frac{1}{V_0 C_T} \int\int \boldsymbol{P}_3 \cdot \boldsymbol{E}_0 \, dz dA \tag{5}$$

and C_T is the output capacity of the transducer. It will be seen that V_{op} tends to be independent of the frequency. Furthermore, as the output capacity C_T is proportional to the length of the output transducer, the *open-circuit output voltage is essentially independent of the transducer length.*

The cross-sectional variations of $\boldsymbol{J}_3$ and $\boldsymbol{E}_0$ are determined by the nature of the acoustic fields, the strength of the nonlinearity, and the nature of the fields associated with the transducer, and can be regarded as invariant over the length of the transducer.

Now let us consider the form of the output from a device of this kind when the two input signals $a_1(t) = F(t) \exp j\omega_1 t$, $a_2(t) = G(t) \exp j\omega_2 t$ are modulated. We choose the frequencies ω_1 and ω_2 so that β_3 corresponds to the period of the output transducer. In this case the open-circuit output signal takes the form

$$V_{op} = B \exp (j\omega_3 t) \int_{-L/2}^{L/2} F(t - z/v_A) G(t + z/v_A - T) \, dz \tag{6}$$

where B is a constant.

If we suppose that the modulated signals exist for a time shorter than the delay time of an acoustic wave along the length of the output transducer, we can take the limits of the integral of (6) as $\pm \infty$ with no loss of generality. It is then convenient to substitute $t - z/v_A = \tau$ so that the output signal finally takes the form

$$V_{op} = v_A B \exp (j\omega_3 t) \int_{-\infty}^{\infty} F(\tau) G(2t - T - \tau) \, d\tau. \tag{7}$$

It will be recognized that a device of this kind yields an output signal which is the convolution of the two input signals compressed in time by a factor of 2, and appears as the modulation of an output signal at a frequency $\omega_3 = \omega_1 + \omega_2$. In most applications this is approximately at double the input frequencies.

The device is flexible and not subject to severe error. For instance, if there is constant attenuation per unit length in the medium, there is no effect on the product $F(t - z/v_A) \exp(-\alpha z)$ times $G(t - z/v_A - T) \exp [-\alpha(v_A T - z)]$, except that its total amplitude is lowered by a factor $\exp -\alpha v_A T$.

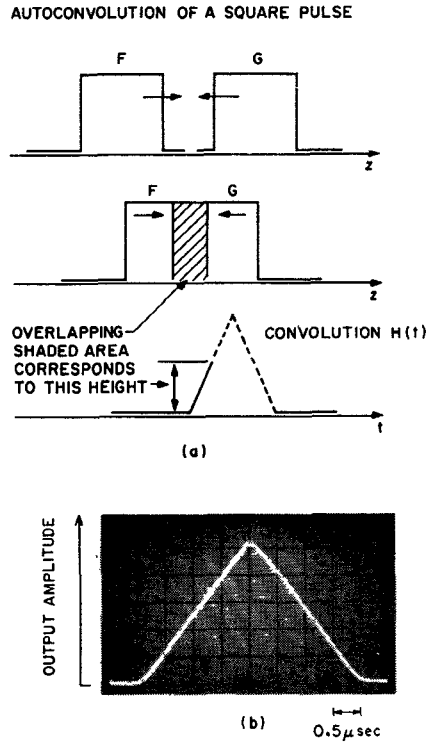

Fig. 4. Autoconvolution of rectangular pulse. (a) As the two acoustic signals pass each other, a triangular output is formed. (b) An actual output signal using the device shown in Fig. 2(c).

It is now worthwhile to consider two simple examples of the types of signals that can be used with this convolution device, remembering, of course, that a wide range of signals can be processed, because $F(t)$ and $G(t)$ can be chosen quite arbitrarily. First let us consider the autoconvolution of a square pulse of length T_p. In this case, the output is a triangular pulse as shown in Fig. 4, whose total time between zero points is just the time it takes the two pulses to pass each other under the output transducer. As their relative velocity is twice the acoustic velocity, the time involved is just T_p. The output waveform is a triangle as would be expected with the convolution process, except that it is time compressed by a factor of 2 and is at a frequency approximately double the input frequencies. The same kind of device can, of course, be used for the convolution of Barker codes, optimum stagger sequences, and other digital codes.

An application which is of some importance, particularly in testing the uniformity of the coupling to the output transducer, is to use an input signal of the form $F(t) = \delta(t)$, i.e., a short pip. In this case the open-circuit output voltage will be of the form

$$V_{op} = v_A D \exp (j\omega_3 t) G(2t - T). \tag{8}$$

Thus the output signal is a reproduction of the input signal, delayed by a time T and time compressed by a factor of 2. If the output transducer coupling is not uniform, it is easy to show from (5) that the output signal will be modulated by the strength of the coupling along the transducer. Such a signal can also be used to give a delayed output where the time delay can be electronically changed by varying the time at which the input pip is introduced.

It is convenient to define a parameter which gives a measure of the efficiency of the device. Several different definitions of such a parameter have been given [13]–[16]. Here we will

call this bilinear conversion factor F_T where

$$F_T = \frac{\mathcal{P}_3}{\mathcal{P}_1 \mathcal{P}_2} \cdot \tag{9}$$

We will also find it convenient to work in terms of internal powers $P_{1\text{ int}}$, $P_{2\text{ int}}$ flowing in an assumed lossless system and define a bilinear conversion factor F_{int} in terms of these powers in the same way as in (9):

$$F_{\text{int}} = \mathcal{P}_3 / \mathcal{P}_{1\text{ int}} \mathcal{P}_{2\text{ int}}. \tag{10}$$

This parameter is of importance when we wish to compare the strength of the nonlinear coupling in different types of devices, without taking account of the conversion efficiency of input transducers or losses. We will often find it convenient to state the values of P_1, P_2, and P_3 in decibels referred to 1 mW, and define F_T and F_{int} in decibels.

The conversion efficiency F_{int} is determined in the main by the properties of the material used, and with the correct design F_{int} is approximately the same for volume and surface-wave devices of the same width w_3. F_T will also depend on losses within the device and the quality of the transducers.

We now consider the situation when two plates are used for the output transducer as shown in Fig. 2(b). In this case with $\omega_3 = 2\omega_1 = 2\omega_2 = 2\omega$ it will be seen that the open-circuit output voltage is of the form

$$V_{\text{op}} = \frac{w_1 h}{w_3 \epsilon_p L} \int\int P_{3y}\, dz dA \tag{11}$$

where $E_0 = V_0/h$, h is the thickness of the crystal, w_1 the width of the acoustic beams, and w_3 the width of the output transducer, assuming $w_3 \geq w_1$. The power densities in the two input signals are $\mathcal{P}_{1\text{ int}}/w_1 h$ and $\mathcal{P}_{2\text{ int}}/w_1 h$, respectively. Hence it follows from (11) that the open-circuit output voltage can be written as

$$V_{\text{op}} = \frac{\kappa}{w_3} (\mathcal{P}_{1\text{ int}} \mathcal{P}_{2\text{ int}})^{1/2} \tag{12}$$

where κ is a constant proportional to the strength of the nonlinear coupling within the medium itself. Whether the medium is used to obtain interactions between surface or between volume waves, κ should not vary much, perhaps by a factor of 2 or 3 at most. However, κ is critically dependent on the choice of material used for the propagating medium. Although the basic source of the nonlinearity is not clearly understood at the present time, κ seems to be largest in the strongly piezoelectric materials such as $LiNbO_3$ and PZT [13].

It will be seen that the open-circuit output voltage depends on the width of the output transducer, the product of the internal input powers, and the strength of the nonlinear coupling. It is essentially independent of the length of the output transducer and the thickness of the piezoelectric crystal. The result will be approximately the same if an interdigital output transducer is used, although the driving current I_{out} will be much larger, because E_0/V_0 is much larger for the interdigital configuration. However, the capacity of the output transducer will also be increased in approximately the same ratio when compared to the parallel-plate output transducer. Also it follows that the output voltage depends only on the input powers, not the power densities.

It is often true that the capacity of the output transducer is relatively large and its reactance at the output frequency relatively small compared to a load resistance R_L of 50 Ω. In this case, the internal efficiency would be

$$F_{\text{int}} = \frac{V_{\text{op}}^2}{2R_L \mathcal{P}_{1\text{ int}} \mathcal{P}_{3\text{ int}}} = \frac{\kappa^2}{2w_3^2 R_L} \cdot \tag{13}$$

The same conclusions apply to the internal efficiency F_{int} as to V_{op}^2, with respect to their variation with the dimensions of the crystal, and the comparison of volume-wave devices with surface-wave devices.

The advantages or disadvantages of using volume or surface waves rests more on other considerations than convolution efficiency. Volume waves are normally more suitable for use at relatively high frequencies. In our case, the volume-wave device is used with input frequencies of the order of 1300 MHz, whereas the surface-wave devices are used with input frequencies in the 100–250-MHz range. Volume-wave devices can handle far higher input powers than surface-wave devices, so they tend to yield a larger dynamic range of operation. On the other hand, surface-wave devices usually have much lower internal and input transducer losses, which leads to a better total conversion efficiency. The time delay per unit length of surface waves is approximately twice that associated with the longitudinal waves used with volume-wave devices of the same material.

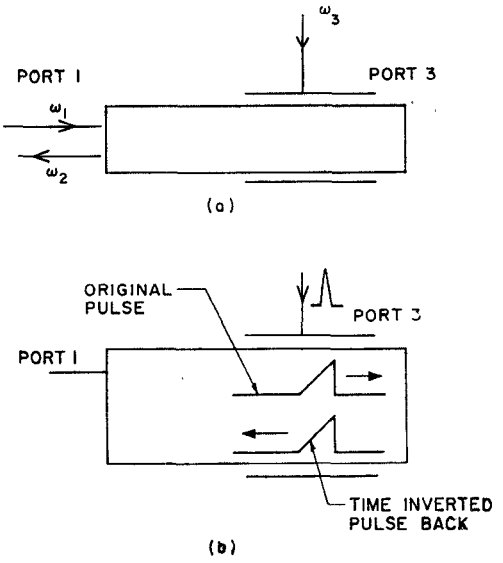

Fig. 5. Diagram of time inversion. The original pulse and the time-inverted pulse are shown spatially separated for illustration purposes. In fact, they propagate through the same part of the crystal. An actual time-inverted signal is shown in Fig. 14. (a) Frequencies which occur. (b) Inversion of a nonsymmetric pulse.

B. *Time Inversion*

We now consider what occurs when an arbitrary signal is inserted in port 1 whose duration is assumed to be less than the time it takes an acoustic wave to pass under the transducer at port 3. The signal applied at port 3 will be a δ-function or short pip. When the input signal arrives under port 3, and the pip signal is introduced, acoustic strain fields are generated in the nonlinear medium at each point x, y, z, which are proportional to the amplitude of the input signal. Because of the phase relations between the pip and the input signal, this generated signal will correspond to an idler which propagates backwards along the device. Consequently, as illustrated in Fig. 5, what was the trailing edge of the original input signal will now arrive at port 1 first, and the front edge of the original input

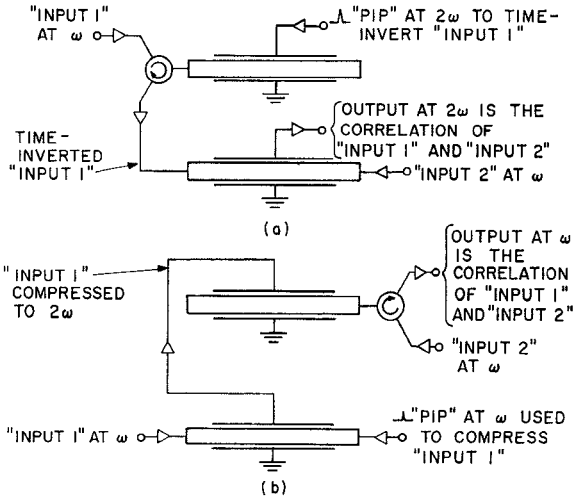

Fig. 6. Methods to *correlate* two input signals using the parametric devices.

signal will arrive back at port 1 last. Thus the input signal will be reproduced inverted in time.

We may put this concept on a more mathematical basis by considering an input signal with a modulation $F(t)$ inserted at port 1 and the corresponding signal inserted at port 3 to have modulation $G(t)$. At any point z and time t, the amplitude of the acoustic component $a_2(t)$ generated at frequency ω_2 will be proportional to $F(t-z/v_A)G(t)$. The output signal modulation arriving back at port 1 must therefore have the form

$$H(t) = \int_{z_0-L/2}^{z_0+L/2} a_2(z, t - z/v_A)\, dz$$
$$= D\int_{z_0-L/2}^{z_0+L/2} F(t - 2z/v_A)G(t - z/v_A)\, dz \quad (14)$$

where z_0 is the coordinate of the center of the transducer at port 3, L its length, and D is a constant depending on the strength of the nonlinear coupling.

We assume, as before, that with short enough signals, we can take the limits of the integral as $\pm\infty$, and with the substitution $t-z/v_A=\tau$, (14) becomes

$$H(t) = Dv_a\int_{-\infty}^{\infty} F(2\tau - t)G(\tau)\, d\tau. \quad (15)$$

The output is related to the correlation of the two input pulses. However, because the argument of $F(t)$ in (15) involves a 2τ, it is not the true correlation. To use this device directly for correlation it would be necessary to take the original signal $F(t)$ and time compress it by a factor of two. This could of course be done as shown in Fig. 6(b).

The other possibility which is shown in Fig. 6(a) uses a pip input $G(\tau)=\delta(T-\tau)$ where T is a time at which the signal corresponding to $F(t)$ is located entirely under the transducer under port 3. In this case

$$H(t) = Dv_AF(2T - t). \quad (16)$$

Thus the output signal is the time inverted form of the input signal $F(t)$ delayed by $2T$. This feature of delay and storage within the device is what enables us to obtain time inversion of the original signal without violating the principle of causality. If the input signal has a bandwidth $\Delta\omega$, the input pip must have a bandwidth of at least $2\Delta\omega$, which implies that its time duration must be less than $\pi/2\Delta\omega$ for accurate time inversion. This implies that, for reasonable bandwidths, the energy in the pulse is small and the output signal will be correspondingly small.

In addition, there is another problem with these devices due to attenuation. The original front edge of the signal, which travels further, will suffer more attenuation than the original lagging edge of the signal. Thus there will be a difference of $\exp -2\alpha v_AT$ introduced between the two ends of the output signal as compared to input signal, where T is the time duration of the signal and α the attenuation per unit length.

III. Parametric Delay-Line Devices

A. Volume Acoustic Wave Devices

In the past, volume-wave delay lines were largely relegated to simple time-delay functions, because there was no practical counterpart of the interdigital tap which allowed one to tap surface-wave delay lines for general signal processing. The parametric process for the first time provides that function in a practical way.

The device in its present form, which is illustrated in Fig. 7, uses two longitudinal waves propagating in opposite directions along the X axis of a 6.2-cm-long (2.5-mm×2.5-mm cross section) $LiNbO_3$ crystal [17]. These waves are excited by ZnO transducers at each end of the crystal. The rectangular $LiNbO_3$ crystal is mounted in a cavity formed by reentrant ridges normal to the y-face of the crystal so as to obtain strong coupling. The electric field of the fundamental cavity mode is therefore essentially confined to the region between the reentrant ridges, and is uniform over the cross section of the crystal. The output transducer consists of a tuned cavity, with a relatively high Q, which is coupled to the external circuit with a loop.

For a cavity with a uniform ridge and uniform walls, the field $E_{0y}(z)$ has a sinusoidal variation along the direction of propagation z. Larson pointed out that, as a result, the convolution integral would be spatially weighted [16]. To prevent this weighting, two rows of tuning screws were installed along the length of the cavity on the side opposite the input loop. These screws perturbed the magnetic field and, as a result, the electric field was lowered in the vicinity of the screws. Also the electric field approaches zero very quickly near the end of the ridges. Fig. 8 shows the effect of the field weighting along the length of the cavity with various adjustments of the screws. These photographs were made using an acoustic probing method; this is a very useful technique because it permits continuous monitoring of the field during adjustment. Since the nonlinear interaction itself is used in this technique, a true representation of the coupling to the electric field along the delay line is obtained.

After the fields within the cavity had been adjusted for uniformity, and the loop adjusted to give a loaded Q of $Q_L\approx 100$ with $\mathcal{P}_1=30$ dBm, $\mathcal{P}_2=35$ dBm, the measured value of $\mathcal{P}_3$ was -38 dBm, so that $F_T=-103$ dB. This device, which operated at input frequencies of 1350 MHz and an output frequency of 2700 MHz, had a net transmission loss for the 1350-MHz signals of 43 dB. Consequently, for comparison purposes, the value of F_{int} for this device with a tuned output load is $F_{\text{int}}=-60$ dB. We estimate that with an untuned output feeding directly into a 50-Ω load, $F_{\text{int}}=-80$ dB.

B. Surface Acoustic Wave Devices

The first surface-wave convolution devices that we constructed used $LiNbO_3$ and operated with input signals of ap-

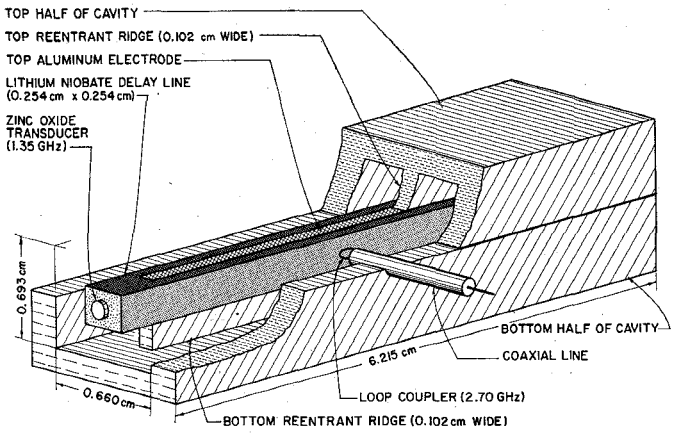

Fig. 7. Cutaway view of bulk-wave convolver showing delay-line crystal clamped between reentrant ridges of output cavity.

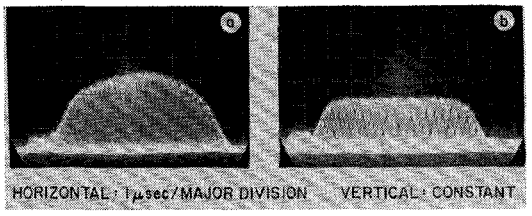

Fig. 8. Weighting of the output coupling due to the shape of cavity E field as shown by the acoustic probing method. (a) Fundamental sinusoidal field of uniform cavity. (b) Uniform coupling with nonuniform cavity.

proximately 105 MHz. Gold or aluminum films were deposited on the top and bottom surfaces of the $LiNbO_3$ to make a $\beta_3 = 0$ output transducer, as illustrated in Fig. 2(b). Typically, the output transducer was 2 cm long and 2 mm wide, the $LiNbO_3$, 1.5 mm thick, and the acoustic beamwidth 1.27 mm. The device had a 10-dB insertion loss between ports 1 and 2, and with a tuned output circuit which gave an 8–10-dB increase in output, the value of F_T was -95 dB; thus $F_{\text{int}} = -85$ dB. It will be seen that F_T is somewhat better than the volume-wave device, but F_{int} is worse than in the volume-wave device, basically because of the higher losses in the output circuit and the fact that a wider output transducer was used. Typically, these devices can be operated with a reference signal $\mathcal{P}_2 = 500$ mW so that $\mathcal{P}_{3\ \text{dBm}} - \mathcal{P}_{1\ \text{dBm}} = -68$ dB and the devices can have a dynamic range of approximately 50 dB when the input signal $\mathcal{P}_1$ is varied.

The device in this form has the disadvantage that one of the input signals, alone, can generate second harmonic components which are observed on the output signal at the time the input signal arrives at the edges of the output transducer. This type of nonlinearity can easily be eliminated by slanting the edges of the top electrode so that they are not parallel to the wavefront [13].

A further problem is associated with reflections from the input transducers. Any signal reflected from one input transducer can convolute with the input signal coming from the other transducer if the delay times are in the right range, thus generating interfering signals.

A good way to eliminate these problems is to use an interdigital output transducer. In this case, a wave reflected from one output transducer is at the wrong frequency to convolute with a wave coming from the other. Furthermore, the device does not respond to a signal at the second harmonic of one of the input frequencies. We have carried out considerable development of such devices, using an interdigital output transducer 2 cm long, with 200 finger pairs, and a periodic spacing of 102 μm. Typically, we have operated with input signals of 195 and 229 MHz, respectively, using appropriate 5 finger-pair input transducers for these frequencies.

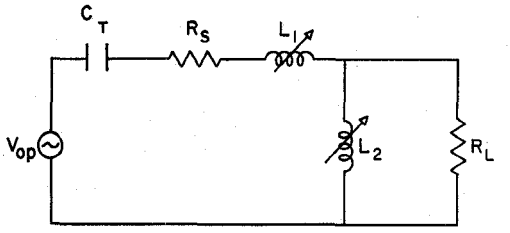

Fig. 9. Schematic of output tuning circuit used with surface-wave device.

The initial experiments with these devices were not encouraging because we observed large transmission losses of the input signals. This was because the fingers of the output transducer shorted out the electric fields associated with the surface waves and scattered them into volume waves. One very successful method of eliminating this difficulty was to space the output transducer from the substrate by 1000–3000 Å. The short wavelength acoustic waves have fields which fall off rapidly away from the substrate, and so their coupling to the output transducer becomes very weak. However, the coupling of the transducer to the product signal, which has a relatively long wavelength, remains essentially unaffected. Two methods for obtaining the required spacing were used. 1) The output transducer was deposited on a separate sapphire substrate, which was pressed down against a 1000-Å SiO spacer deposited on the $LiNbO_3$ substrate, leaving an air gap between the transducer and the $LiNbO_3$ surface, as in our earlier amplifier devices. 2) A monolithic device was constructed by depositing the output transducer on top of a layer of vacuum deposited SiO or RF sputtered SiO_2 on the $LiNbO_3$ substrate. In the first case, the excess transmission loss due to the presence of the output transducer was negligible; in the second case, too thick a layer of the dielectric gave rise to acoustic losses within it, and too thin a layer caused losses due to the presence of the transducer. With the optimum thickness of RF sputtered SiO_2, the best material for the purpose, the loss could be reduced to 2 dB (1 dB/cm) at 220 MHz, yielding values of $F_T = -81$ dB with $F_{\text{int}} = -66$ dB in a tuned output circuit. The results with the air-gap device were approximately the same; but it has the disadvantage of requiring strict mechanical tolerances and precision alignment. On the other hand, its use in a time-inversion device is, at the moment, preferable, because of its extremely low loss.

Usually, the output transducer was placed in a tuning circuit, which gave an improvement in efficiency of the order of 10 dB without decreasing the bandwidth of the device to less than the 30-MHz bandwidth of the input transducers [5]. The tuning circuit shown in Fig. 9, consisting of a tapped inductance with a variable tap length and a variable inductance, was used to tune out the capacitance of the output transducer and to match it to a 50-Ω load. The tuning device we used consisted of a shorted stripline with a variable tap along it; the length of the line was variable as was the position of the tap. The output bandwidth was not limited by output tuning, but only by the bandwidth of the input transducers. We estimate from our results that the effective series resistance present was as much as 0.6 Ω and the capacitive reactance $1/\omega_3 C_T$ was 4.7 Ω.

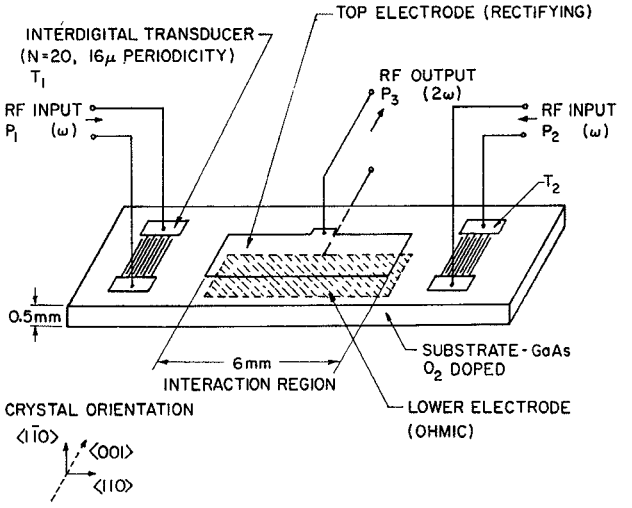

Fig. 10. GaAs device which uses the semiconducting properties of the piezoelectric to obtain higher output efficiency.

It will be seen, then, that as a convoluter with $F_T = -81$ dB, a loss $\mathcal{P}_{3\ \mathrm{dBm}} - \mathcal{P}_{1\ \mathrm{dBm}} = -61$ dB is obtained with a 20-dBm reference signal. This gives a dynamic range of approximately 50 dB with the input signal limited to 20 dBm.

C. Surface-Wave Acoustic Devices with Semiconductor Interactions

We have increased the efficiency of parametric devices by employing the nonlinear response of a semiconductor coupled to the RF fields associated with the acoustic waves propagated along a piezoelectric delay line. Two types of interactions with semiconductors are possible: longitudinal interactions in which the nonlinearity is caused by a field parallel to the direction of propagation, and transverse-field interactions caused by a field perpendicular to the direction of propagation [8], [11], [18]. The first type has the disadvantage, as first pointed out by Wang [2], that the output is obtained only when a drift field is applied to the semiconductor. In this case, the attenuations of the two waves propagating in opposite directions through the devices are different, and so the convolution output signal will be distorted.

We shall therefore concentrate on the transverse-field interaction devices, which do not need an applied drift field, and so do not distort the output signal.

1) Devices Using Piezoelectric Semiconductors: An approach to which we have devoted a great deal of attention involves the use of delay lines constructed of GaAs, a material which is semiconducting as well as piezoelectric. This material has a weak piezoelectric coupling coefficient, but is an excellent semiconductor with a low carrier density and high mobility, resulting in a high nonlinear coupling strength. Using a Bleustein–Gulayev wave, a type of surface shear wave with a large penetration depth [19], [20], results comparable to those obtained on $LiNbO_3$ devices have been obtained. Also, by using Rayleigh waves on GaAs, results of the same order of magnitude have been obtained.

We have considered the parametric interactions which can occur in a material like GaAs in the configuration shown in Fig. 10. In this case, the device is degenerate, and the output transducer consists of two metal films on the upper and lower surfaces of the crystal; the top film is normally a Schottky barrier and the lower film an ohmic contact [8]. Interdigital transducers are normally used to excite the acoustic waves.

The basic cause of the nonlinearity is associated with the relation between current and field in the semiconductor medium:

$$\boldsymbol{J} = \mu\rho\boldsymbol{E} = \mu\boldsymbol{E}\nabla\cdot\boldsymbol{D}. \tag{17}$$

In a weak piezoelectric coupling medium, both the electric field $\boldsymbol{E}$ and the displacement density $\boldsymbol{D}$ are proportional to the applied strain fields, so that there is always a second-order product term contained in the current density. When (17) is solved to first order in conjunction with the equation of conservation of charge, and the constitutive relations between stress, strain, and electric field, the dispersion relation for the fields which propagate through the medium in the presence of the mobile carriers is obtained. From this relation it can be shown that the loss per unit length of the acoustic waves in the medium is [21]

$$\alpha = K^2 \frac{\omega_c/2v_A}{1 + (\omega_c/\omega)^2} \tag{18}$$

where $\omega_c = \mu\rho_0/\epsilon$ is the dielectric relaxation constant of the medium, ρ_0 the carrier charge density, and K^2 is the piezoelectric coupling constant. For a surface shear wave or even for a Rayleigh wave, K^2 closely approximates the value for a plane shear wave.

When the same equations are solved to second order in the field quantities, it can be shown that the open-circuit output voltage V_{op} due to two oppositely directed surface shear waves with power flows $\mathcal{P}_1$, $\mathcal{P}_2$, respectively, at each end of the device is given by the relation

$$|V_{op}| = \frac{\mu K^2}{w_3 \epsilon v_A^2} \frac{(\omega_c/\omega)\exp(-\alpha L)}{[(\omega_c/\omega)^2 + 1][(\omega_c/\omega)^2 + 4]^{1/2}} \cdot (\mathcal{P}_1\mathcal{P}_2)^{1/2} \tag{19}$$

where L is the length of the crystal between the input terminals.

It will be seen from this result that the output voltage, and hence the efficiency of the device, depends on the product μK^2. The use of a high-mobility semiconductor can therefore compensate for a relatively weak coupling coefficient. On this basis, GaAs would appear to be one of the better choices for the piezoelectric semiconductor required.

Optimum efficiency is obtained in these devices by adjusting the conductivity of the material, and hence ω_c to maximize the output power. For low loss, this occurs where $(\omega_c/\omega) \approx 1$. However, as the loss of the input signals (the $\exp -\alpha L$ term) is usually the most important term, optimum efficiency is normally obtained with $(\omega_c/\omega) \ll 1$.

With the structure shown in Fig. 10, we take $K^2 = 0.004$ for a surface shear wave, $v_A = 3.34 \times 10^5$ cm/s, $\mu = 6000$ cm^2/V·s, $L = 0.6$ cm, $w_3 = 1.7$ mm, and $h = 0.05$ cm. With these values we find that for a frequency of 205 MHz, after estimating the losses, F_{int} lies between -60 to -47 dB, and the optimum dielectric relaxation frequency is where $\omega_c/\omega = 0.08$. This corresponds to a resistivity of approximately 800 Ω·cm. In the experiments, we used bulk GaAs which could be heated or cooled to give the required resistivity. The results obtained at the point of maximum efficiency were found to be $F_T = -94$ dB. The transducer loss was approximately 49 dB, so this corresponded to a value of F_{int} of -45 dB, a value close to the best theoretical prediction.

It will be seen that despite the very small value of K^2 in GaAs, and the poor coupling into the device, F_{int} is much

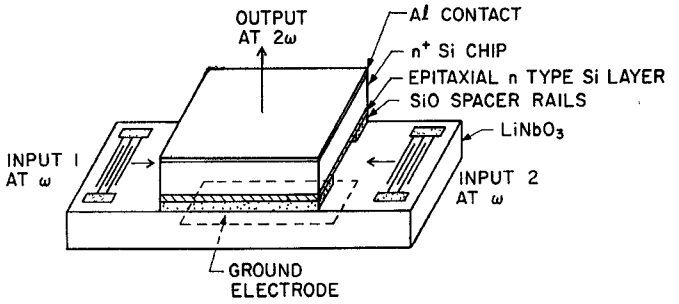

Fig. 11. Separated-medium device which combines the good semiconductor properties of Si with the strong piezoelectric properties of $LiNbO_3$.

larger than for $LiNbO_3$ and F_T is comparable in value. Consequently, the effect of the semiconductor nonlinearity is very strong compared to the nonlinearity in $LiNbO_3$. As a large part of these losses are due to poor transducer efficiency, and since techniques are available for decreasing these losses, it is entirely possible that GaAs devices will become useful high-efficiency convoluters in the future.

2) Separated Medium Devices: Ideally, what is required is a material which is both a good semiconductor and has a strong piezoelectric coupling coefficient. To satisfy these needs, we have used a semiconductor located close to a $LiNbO_3$ substrate on which acoustic surface waves are propagating, and have obtained efficiencies over 30 dB greater than in the corresponding surface-wave devices. A schematic of the configuration used is shown in Fig. 11. With this configuration both the longitudinal component of field in the direction of acoustic propagation and the transverse component of field, normal to the surface of the semiconductor, could interact with the carriers in the semiconductor. For the reasons already given, we have tried to work exclusively with transverse interactions.

In most cases, it is found that the acoustic loss can be minimized by using a semiconductor with a resistivity on the order of 10 Ω·cm. With very high resistivity materials, the losses due to the interaction of the longitudinal component of the wave with the semiconductor may be excessively high. However, as we shall show, the higher the resistivity the stronger the nonlinear coupling. So a compromise is required in the choice of resistivity, at least for use in convoluters.

The basic interaction process with which we are concerned is one in which the semiconductor behaves like a distributed varactor. A simple physical explanation of the cause of the nonlinearity may be arrived at by considering that the RF fields of the acoustic wave give rise to a normal field component E_n at the surface of the semiconductor. A depletion layer of thickness l_d forms, where

$$E_n = \frac{qN_d l_d}{\epsilon} \tag{20}$$

and N_d is the donor density, and ϵ the permittivity of the semiconductor. The potential ϕ_d generated across the depletion layer will therefore be

$$\phi_d = \frac{qN_d l_d^2}{2\epsilon} = \frac{E_n^2 \epsilon}{2qN_d} . \tag{21}$$

Thus it will be seen that the potential is proportional to the square of the field which is the basic cause of the nonlinearity.

The physical picture we have given so far is somewhat oversimplified, because with the RF fields normally used, the depletion layer that is formed at the surface of the semiconductor is less than the Debye length, $\lambda_d = (kT\epsilon/q^2N_d)^{1/2}$, where T is the temperature of the semiconductor. When the theory is modified to take this effect into account, it is found that the potential developed across the depletion layer is

$$\phi_d = \frac{E_n^2 \epsilon}{6qN_d} . \tag{22}$$

Thus the only difference between this result and the earlier one obtained by using a simplified physical picture is a factor of 3. Note that temperature drops out of the final expression.

If we now assume that the acoustic waves have fields associated with them of the form $E_1 \exp j(\omega t - \beta_1 z)$, $E_2 \exp j(\omega t + \beta_2 z)$, respectively, we can relate E_1 and E_2 to the incident powers, and carry out a derivation much like the one given in Section II to determine V_{op}. Assuming zero loss, we find that

$$V_{op} = \frac{8}{3qN_d} \frac{\epsilon_0 + \epsilon_p}{\left(1 + \frac{\epsilon_p}{\epsilon'} \beta_A h\right)^2 \epsilon} \left|\frac{\Delta v}{v}\right| \frac{\omega}{v_A^2 w_3} \cdot (\mathcal{P}_{1\,\mathrm{int}} \mathcal{P}_{2\,\mathrm{int}})^{1/2} \tag{23}$$

where h is the thickness of the gap between the semiconductor and the acoustic medium, ϵ' the permittivity of the material in the air gap, ϵ_p the effective permittivity of the piezoelectric substrate, w_1 the acoustic beamwidth, w_3 the width of the output transducer, $\Delta v/v$ the relative change in acoustic wave velocity when a perfect conductor is placed at the surface of the acoustic medium, and $\beta_A = \omega/v_A$.

It will be seen from this relation that it is desirable to work with as low a carrier density as possible, provided that the transmission loss does not become too high, for V_{op}^2 and hence F_{int} vary as $1/N_d^2$. Similarly, as V_{op} is proportional to $\epsilon_0 + \epsilon_p$ when $h = 0$, it is desirable to use a piezoelectric material with ϵ_p and $\Delta v/v$ as large as possible, but with v_A^2 as small as possible. Thus it would appear that $Bi_{12}GeO_{20}$ might be as good a choice for the substrate material as $LiNbO_3$, because $(\epsilon_0 + \epsilon_p)(\Delta v/v)/v_A^2$ for $Bi_{12}GeO_{20}$ (1.5×10^{-22}) is slightly larger than for $LiNbO_3$ (1.3×10^{-22}). As the acoustic loss due to the presence of the semiconductor would be lower with $Bi_{12}GeO_{20}$, and the delay times obtainable for a given length almost twice as large, $Bi_{12}GeO_{20}$ would appear to be a desirable choice of material for this purpose.

In the first device we tested, we used a 5000-Å-thick layer of InSb deposited on top of a 300-Å layer of SiO laid down on the $LiNbO_3$. InSb has the disadvantage of a relatively high carrier density, in this case 2×10^{17} cm^{-3}. With this device there was no noticeable increase in transmission loss due to the presence of the InSb, and we obtained an improvement of 8 dB in F_T over the equivalent parallel-plate device, corresponding to a tuned value of $F_T = -85$ dBm. This compares quite closely to the theoretical (untuned) figure of $F_T = -88$ dBm.

In experiments with silicon with 105-MHz input frequencies, we used 10-Ω·cm bulk material, which had a 2-Ω resistance between the back electrode and the front surface, spaced by 1000 Å from the $LiNbO_3$ with an SiO_2 spacer as illustrated in Fig. 11. We found that the excess loss due to the presence of the semiconductor was 5 dB, with $F_T = -64$ dBm and $F_{int} = -47$ dBm.

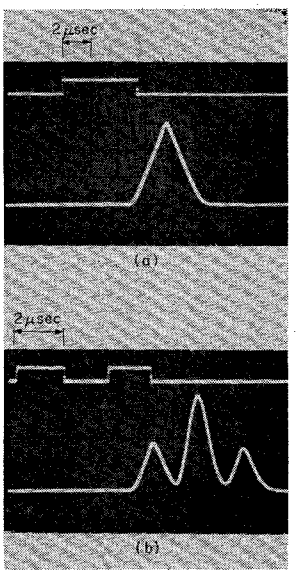

Fig. 12. Autoconvolution of single and double rectangular pulses using the device shown in Fig. 11. The upper trace in each photograph is the input. The lower trace is the output in each case.

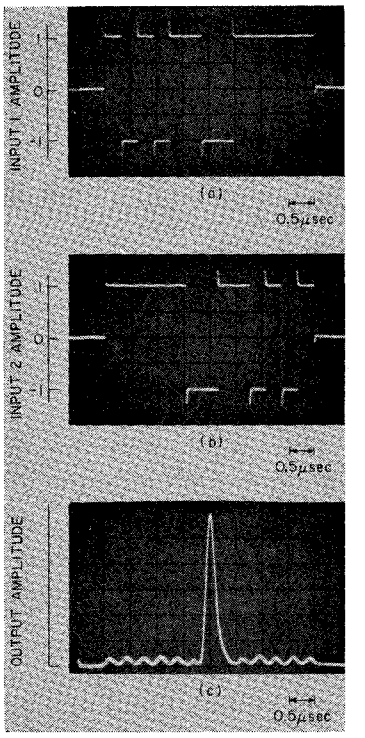

Fig. 13. Autocorrelation of 13-bit Barker code obtained with the device shown in Fig. 2(c). (a) Input 1. (b) Input 2. (c) Output.

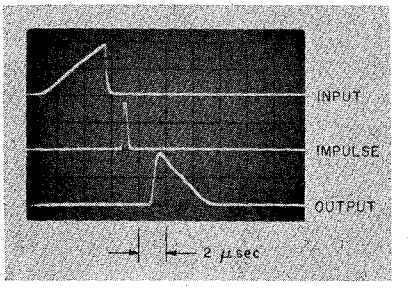

Fig. 14. Time inversion of nonsymmetric pulse using the device shown in Fig. 2(c).

In order to avoid resistive losses, it seemed that it would be advisable to work with as thin a layer as possible of n-type material, as suggested by Otto and Moll [10], laid down on an n+ substrate. With a layer sufficiently thin, the propagation loss would be reduced by a factor $\tanh(2\pi d/\lambda)$ where d is the thickness of the layer and λ the acoustic wavelength. In addition, by using epitaxial material, the series resistance due to the use of high-resistivity bulk material of finite thickness would be essentially eliminated. So far we have not been able to work with material sufficiently thin to reduce the propagation losses. This would require material of the order of 1 μm thick to reduce the loss by a factor of 5 at 100 MHz. However, by working with layers approximately 7 $\Omega\cdot$cm and 5–8 μm thick, at a 105-MHz input frequency, we have obtained a nonlinear conversion factor of $F_T = -52$ dB with a tuned output corresponding to $F_{\text{int}} = -49$ dBm and $F_T = -60$ dBm when working directly into a 50-Ω untuned load. The excess loss due to the presence of the semiconductor was only 2 dB.

In all cases measured, the experimental values of F_T were always within a few decibels of the theoretical predictions.

It will be seen that these results are 29 dB better than those obtained in the equivalent $LiNbO_3$ convoluter with an interdigital output transducer, and 43 dB better than with the equivalent device with a parallel-plate output transducer. With a 20-dBm reference signal, the implication is that the output power $\mathcal{P}_3$ would only be 32 dB less than the input power, a performance figure which makes this device applicable to a wide range of signal-processing systems.

D. Experimental Signal-Processing Parametric Devices

We have tested the signal-processing capability of the parametric convolution devices with both analog and digital signals. In this section, we shall give some examples of the results obtained. In most cases, the results are in excellent agreement with what would be expected theoretically.

As a simple example, the autoconvolution of rectangular pulses is shown in Fig. 12, using both single and double pulses. These results were obtained with the separated semiconductor device shown in Fig. 11. The convolution output is of the correct form with triangular output waveforms. The amplitude of the output signal varies linearly with the time duration of the input pulses, as would be expected from theory.

We have demonstrated the convolution of various types of digital codes in all these devices [5], [22]. As an example, Fig. 13 shows the autocorrelation of a 13-bit biphase Barker sequence 5 μs long consisting of 0.38-μs pulses obtained with the interdigital transducer output transducer device of Fig. 2(b). Barker sequences have the property that their matched filter response consists of a correlation peak with amplitude corresponding to the number of bits in the code and relative sidelobe levels of -1, 0, and $+1$ only. Because of the phase cancellations necessary to obtain these sidelobe levels, the requirements of uniformity of interaction on the device employed are quite stringent. The outputs illustrated in the figure show the device is performing well. The sidelobes are at the proper level although there is some distortion of the sidelobe following the peak.

Fig. 14 shows the results obtained from this system when it is used for time inversion [5]. In this case, a narrow pip 0.1 μs long at 3-dB points with a carrier frequency of 424 MHz

was fed into the device through the tuner on the center transducer. The input power to the pip was approximately 2 W. An unsymmetrical triangular pulse 5 μs long of 25 dBm was fed into the input transducer at 196 MHz; the output signal was taken out on a separate transducer tuned to 230 MHz. It will be seen that a time-inverted signal is generated. There are slight distortions in the signal output due to nonuniformities in the center transducer and its separation from the $LiNbO_3$, and the rise time of the pulse was deteriorated so that the fall time of the time reversed pulse was increased by twice the length of the pip, as would be expected. The output signal was -65 dBm, so the loss from input to output was 90 dB. The measured value of $\mathcal{P}_{1\text{ dBm}}-\mathcal{P}_{2\text{ dBm}}-\mathcal{P}_{3\text{ dBm}}$ was -123 dB, and the dynamic range is less than 25 dB. The value of efficiency obtained checks well with the efficiency of $F_T=-81$ dBm of the same device as a parametric convoluter. It can be shown from the Manley–Rowe relations that the efficiency should be reduced by a factor of $(T_{\text{pip}}/T_3)^2(\omega_1\omega_2/\omega_3^2)$ (see [12]). With $T_{\text{pip}}=0.1$ μs, $T_3=5.6$ μs, we find that $\mathcal{P}_1/\mathcal{P}_2\mathcal{P}_3=-122$ dB, a value within 1 dB of the experimental figure.

It has not been possible to obtain time inversion in a simple parallel-plate acoustic surface wave convoluter using acoustic nonlinearities, because of its poor efficiency, although time inversion has been observed in the volume-wave device [17]. Time inversion has also been demonstrated in the separated semiconductor device, the result being of the order of 35 dB worse than when the device is used as a convoluter, as would be expected. So far, because of the loss within the semiconductor region, the device has not given an output which is an accurate time-inverted version of the input signal. However, we expect that in the future we shall be able to reduce the losses of these devices, and if necessary taper the gap between the semiconductor and the piezoelectric medium so as to increase the nonlinear coupling along the device to compensate for losses.

The pure surface-wave, semiconductor surface-wave, and volume-wave devices have also been used to give pulse compression of FM chirp signals. Pulse compression makes it necessary, in principle, to use a chirp input at each end of the device, one of which has a frequency increasing with time, the other decreasing with time, i.e., one signal must be the time-inverted version of the other. In principle, this could be done by passing one of the chirp signals through a time inverter first. However, as we have seen the present time-inversion devices have very weak or inaccurate outputs. As the more efficient semiconductor parametric devices come into use, we would expect this difficulty to be eliminated. Meanwhile, we decided to demonstrate the principle of pulse compression by using the so-called *V*-chirp.

For the experiments with volume-wave devices, which will be described here, the input signal was gated on for 7 μs, and swept from frequency $f_{\min}$ to frequency $f_{\max}$ and back to $f_{\min}$ in this time. The convolved outputs for several values of $\Delta f=|f_{\min}-f_{\max}|$ are shown in Fig. 15.

Since the input signal is the same as the constant-length reference signal, the output peak level should not be a function of Δf until Δf exceeds the bandwidth of the system. The compressed main lobe of a constant amplitude (no weighting), linear FM chirp should have a 3-dB width $t_{3\text{dB}}=0.44/\Delta f$. If the amplitude of the input or reference chirp is varied as a function of frequency, as with Hamming or Gaussian weighting [23], the pulse should become wider and lower by the amounts given in Fig. 16.

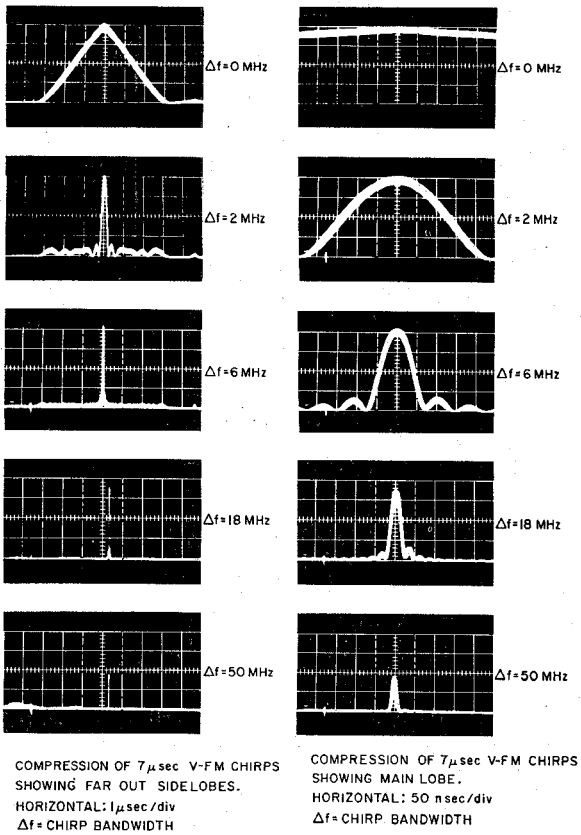

Fig. 15. Pulse compression obtained with the device shown in Fig. 7.

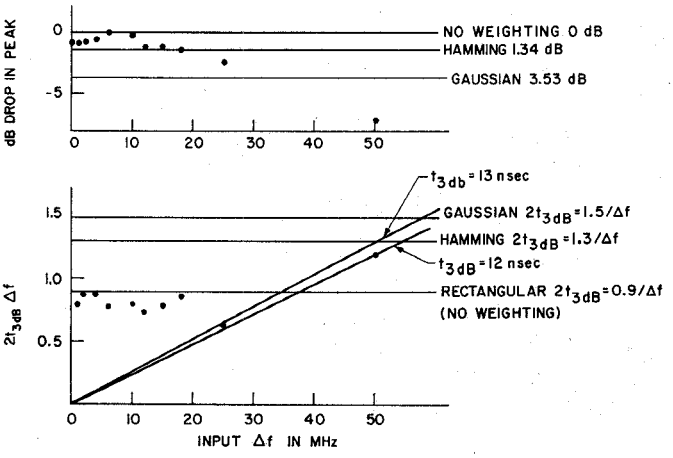

Fig. 16. Results from compressed signals as input signal bandwidth is increased. Upper plot shows relative level of main peak versus Δf. Lower plot describes behavior of the 3-dB width in time $t_{3\text{dB}}$ for various values of Δf.

If the bandwidth of the system is $\Delta f_{3\text{dB}}$, then the narrowest pulse that can be observed will have a timewidth $2t_{3\text{dB}}\approx(2.9\Delta f_{3\text{dB}})^{-1}$. If the bandwidth is increased beyond this point, the energy associated with the frequencies outside the band is rejected. Thus, for excessive bandwidths, the amplitude of the compressed peak should become significantly reduced and $2t_{3\text{dB}}\Delta f$ should approach the constant slope value $\Delta f/(2.9\Delta f_{3\text{dB}})$.

It can be seen that, based upon the time duration and usable bandwidth of the *input* signal, time–bandwidth products well in excess of 100 are obtained before limitation by the bandwidth of the system occurs.

IV. Conclusions

Parametric devices have been shown to give accurate convolution of modulated RF signals. The first devices of this kind made use of the nonlinearities in the acoustic medium itself. This is a relatively weak nonlinearity which yields conversion efficiencies of the order of 60–80 dB with a parametric signal of 20 dBm. Even so, this gives output signals 40–50 dB above the noise level in devices with a bandwidth of the order of 30 MHz and delay time of the order of 6 μs, and hence a time–bandwidth product of approximately 200. With such devices, real-time convolution, pulse compression, and time inversion of signals have been obtained.

Volume-wave devices have the advantage over surface-wave devices that they can be operated at higher input power and are suitable for use at higher frequencies; the present ones operate with an L-band input signal. On the other hand, surface-wave acoustic devices are easier to construct in the 50–300-MHz input frequency range for long time delays and large time–bandwidth products. Their efficiency, in practice, tends to be somewhat better than the volume-wave devices, although it is not clear that this is necessarily so.

All of these devices have the great advantage that they are electronically programmable, for they use as a reference another signal rather than a fixed filter. The devices operate in real time; therefore, they can perform functions which are difficult or impossible to perform by any other technique. One prime example is the possibility of taking the autocorrelation of a received signal. Even if such a signal has been distorted during its passage along a long path from the transmitter, its autocorrelation can still be taken and important features of the signal pattern recognized. For instance, a radar signal transmitted through the ionosphere may be badly distorted. By taking the signal's autocorrelation, features of an object can still be recognized despite the distortion.

In all cases it would be desirable for the parametric devices to have as high an efficiency as possible. In our opinion, the most fruitful line of attack on this problem is to employ the nonlinear properties of a semiconductor. In particular, the use of transverse-field interactions, with the semiconductor behaving essentially as a distributed varactor, has already improved the output efficiency over the equivalent $LiNbO_3$ devices by 30–40 dB and holds the promise of considerably greater improvements. The present semiconductor devices are already providing high performance with an output only 32 dB below the input signal with a reference signal of 100 mW, and with bandwidths determined essentially by the input transducers. Their disadvantage is that they use a semiconductor supported by spacer rails only a few hundred angstroms away from the piezoelectric substrate. It would be far more desirable to use a monolithic device. The inherent loss due to the presence of the semiconductor only decreases the convolution output, but does not distort the output signal. However, this loss does contribute to distortion when the device is used for time inversion, although the output is now much larger than in devices which operate with a purely acoustic nonlinearity. The loss due to the semiconductor is, in fact, comparable to that obtained in our present monolithic devices which employ an acoustic nonlinearity and have an interdigital output transducer. We believe that we can eliminate this difficulty by tapering the spacing between the semiconductor and the $LiNbO_3$.

We are at present pursuing methods for making high-efficiency monolithic devices. The approach being employed is to deposit ZnO, a piezoelectric material with a relatively high coupling coefficient, directly onto silicon or GaAs. With GaAs this should make it possible to fabricate relatively efficient input transducers, so as to make the GaAs convolution devices as efficient as the present spaced $LiNbO_3$–Si system. With silicon, a ZnO layer deposited on it would be used to provide coupling both for the input and the output transducers. In this case, with a ZnO film RF sputtered directly onto silicon, an interdigital output transducer could be used so as to avoid the problem of having the output frequency at the second harmonic of the input frequency.

Thus output efficiencies have been obtained in these devices close to the figures obtained in fixed systems. The efficiency should become still better in the near future, making it possible to use these devices and their great flexibility in a wide variety of systems. The best devices at the present time are not monolithic. Active development of monolithic devices is being pursued, and they should become a reality within the near future, with output efficiencies comparable to the present spaced medium devices.

Acknowledgment

The authors wish to thank the Center for Materials Research, Stanford University, for the single crystal materials which they supplied; H. Gautier, N. J. Moll, and O. W. Otto for some of the more recent measurements on semiconductor interactions; and C. F. Quate for many helpful discussions.

References

[1] L. O. Svaasand, "Interaction between elastic surface waves in piezoelectric materials," *Appl. Phys. Lett.*, vol. 15, pp. 300–302, 1969.
[2] W. C. Wang, "A novel ultrasonics oscillator and convolution integrator," presented at the Joint Services Technical Advisory Commit. Meet., Polytechnic Institute of Brooklyn, Brooklyn, N. Y., 1966; also, W. C. Wang and P. Das, "Surface wave convolver via space charge nonlinearity," in *Proc. 1972 Ultrasonics Symp.*, pp. 316–321, Oct. 1972.
[3] C. F. Quate and R. B. Thompson, "Convolution and correlation in real time with nonlinear acoustics," *Appl. Phys. Lett.*, vol. 16, pp. 494–496, June 15, 1970.
[4] M. V. Luukkala and G. S. Kino, "Convolution and time inversion using parametric interactions of acoustic surface waves," *Appl. Phys. Lett.*, vol. 18, pp. 393–394, May 1, 1971.
[5] W. R. Shreve, G. S. Kino, and M. V. Luukkala, "Surface wave parametric signal processing," *Electron. Lett.*, vol. 7, pp. 764–766, Dec. 30, 1971.
[6] J. M. White, D. K. Winslow, and H. J. Shaw, "Variable bandwidth frequency modulation chirp pulse compression using a longitudinal acoustic wave convolver at 1.3 GHz," *Electron. Lett.*, vol. 8, pp. 446–447, Aug. 24, 1972.
[7] I. M. Mason, M. O. Motz, and J. Chambers, "Parametric interaction of acoustic surface wedge wave," *Electron. Lett.*, vol. 8, pp. 429–430, Aug. 24, 1972; also, P. E. Lagasse, I. M. Mason, and E. A. Ash, "Acoustic surface waveguides—Analysis and assessment," this issue, pp. 225–236.
[8] S. Ludvik and C. F. Quate, "Nonlinear interaction of acoustic surface waves in epitaxial gallium arsenide," unpublished.
[9] G. S. Kino, W. R. Shreve, and H. R. Gautier, "Parametric interactions of Rayleigh waves," in *Proc. 1972 IEEE Ultrasonics Symp.*, pp. 285–287, Oct. 1972.
[10] O. W. Otto and N. J. Moll, "A lithium niobate silicon surface wave convoluter," *Electron. Lett.*, vol. 8, pp. 600–602, Nov. 30, 1972.
[11] C. W. Lee and R. L. Gunshor, "Enhancement of nonlinearity in surface acoustic wave propagation from coupling to charge carriers," *Appl. Phys. Lett.*, vol. 7, pp. 696–697, 1971.
[12] M. Chodorow and C. Susskind, *Fundamentals of Microwave Electronics*. New York: McGraw-Hill, 1964.
[13] E. A. Kraut, T. C. Lim, and B. R. Tittmann, "Application of nonlinear interactions in ferroelectric ceramics to microwave signal processing," *IEEE Trans. Sonics Ultrason. (Special Issue on the Applications of Ferroelectrics)*, vol. SU-19, pp. 247–255, Apr. 1972.
[14] M. Luukkala and J. Surakka, "Acoustic convolution and correlation and the associated nonlinearity parameters in $LiNbO_3$," *J. Appl. Phys.*, vol. 43, pp. 2510–2518, June 1972.
[15] R. B. Thompson and C. F. Quate, "Nonlinear interaction of microwave electric fields in $LiNbO_3$," *J. Appl. Phys.*, vol. 12, pp. 907–919, Mar. 1, 1971.
[16] J. D. Larson, III, "Acoustic wave generation by piezoelectric plates and films," Ph.D. dissertation, Stanford Univ., Stanford, Calif.

[17] J. M. White, D. K. Winslow, and H. J. Shaw, "Time reversal and correlation at 1.35 GHz using nonlinear interaction in a bulk acoustic-wave device," *Proc. IEEE* (Lett.), vol. 60, pp. 1102–1103, Sept. 1972.
[18] M. Yamanishi and T. Kawamura, "Acoustic-surface wave convolver using nonlinear electron interactions in coupled semiconductor-piezoelectric systems," in *Proc. 1972 IEEE Ultrasonics Symp.*, pp. 288–291, Oct. 1972.
[19] J. L. Bleustein, "A new surface wave in piezoelectric materials," *Appl. Phys. Lett.*, vol. 13, pp. 412–413, Dec. 15, 1968.
[20] Yu. V. Gulayev, "Electroacoustic surface waves in solids," *JETP Lett.*, vol. 9, no. 37, Jan. 5, 1969.
[21] A. R. Hutson and D. L. White, "Elastic wave propagation in piezoelectric semiconductors," *J. Appl. Phys.*, vol. 33, pp. 40–47, Jan. 1962.
[22] D. K. Winslow, H. J. Shaw, and J. M. White, "Acoustic parametric interactions," Stanford Univ., Stanford, Calif., Semiannu. Rep. F30602-71-C-0125, Microwave Lab. Rep. 2108, Oct. 1972.
[23] C. E. Cook and M. Bernfeld, *Radar Signals—An Introduction to Theory and Application*. New York: Academic Press, 1967, p. 197.

Signal Processing by Electron-Beam Interaction with Piezoelectric Surface Waves

ALAIN G. BERT, BERNARD EPSZTEIN, AND GÉRARD KANTOROWICZ

Abstract—**A new type of device is described in which an acousto-electric surface wave interacts with low energy free charges created on the surface of a piezoelectric material. The experimental results obtained show that one of the most promising applications is an analog RF storage device for which several minutes of storage time have been achieved at 30 MHz on quartz with an internal insertion loss of 63 dB. If the width of the current pulse is large enough, direct attenuation of the surface wave may be measured due to the energy absorbed by the motion of secondary electrons. Experimental and theoretical results are presented. The limitations and the applications of the device to signal processing are discussed.**

I. Introduction

BULK and surface acoustic waves are both used in signal processing, but surface waves are generally more versatile because of their accessibility. This feature is particularly important on piezoelectric substrates: the wave can be coupled to the external medium through the electric field associated with it. We discuss here some interactions between the electric field and free charges moving in vacuum near the surface. The free charges may be created either by a cathode (or photocathode) or by secondary emission. In any case their mean energy must be small, i.e., of the order of magnitude of the potential associated with the acoustic wave, in order to allow the electric field of the wave to modify the trajectories of the primary or secondary electrons and/or to change the amount of created charges. Three kinds of devices can be derived from this principle.

1) By processing the resulting current modulation, one may use the device as an electronic acoustic wave transducer.

2) When the resulting modulation of the charge density is made to create an electrostatic image of the acoustic wave on an insulating surface, which may be the surface of the piezoelectric substrate itself, the device will be able to store the acoustic signal and achieve associated functions, such as time inversion.

Manuscript received October 4, 1972; revised November 3, 1972. This work was supported in part by the Direction des Recherches et Moyens d'Essais, Paris, France, under Contract 71/194.

The authors are with the Laboratoire de Recherches Hyperfréquences, Groupement Tubes Electroniques, Thomson-CSF, Orsay, France.

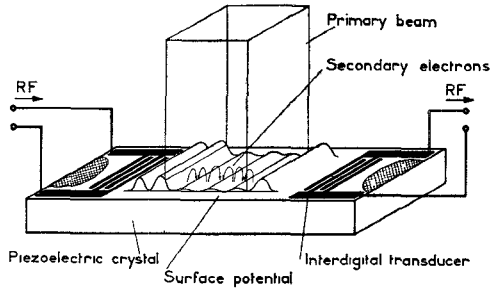

Fig. 1. Schematic diagram of acoustic signal storage device.

3) Cumulative interaction between the electric potential of a surface wave and adjacent free electrons can produce either an attenuation or an amplification on an acoustic wave.

Examples of the first type of devices have been given by a number of authors. The detection of a piezoelectric field by modulation of secondary electrons emitted by an electron beam of a few hundred volts impinging on a piezoelectric plate immersed in an acoustic field, is used in the Sokolov ultrasonic camera [1] for visualization of an acoustic field.

Electron-beam sensing of a surface elastic wave has been considered in order to provide an electronically variable delay line [2], but the results published up to now have not yet proved whether this approach could be successful.

The present paper is primarily concerned with the two other types of devices for which first experimental results have been given in a recent paper [3]. A schematic diagram of the operation is given in Fig. 1. An electron beam accelerated at a few hundred volts is made to impinge upon the entire surface of a piezoelectric crystal. Its current density may be varied from zero to tens of milliamperes per square centimeter. Input and output interdigital transducers are deposited on the surface. The beam current is pulse modulated. A metallic shield prevents electrons from hitting the fingers of the transducers. After an RF signal has been fed through the input transducer, the surface is flooded by the electron beam during a few nanoseconds. After a delay which may be as long as 1 min, the